NASA Technical Memorandum 4285

A Compensatory Algorithm for the Slow-Down Effect on Constant-Time-Separation Approaches

Terence S. Abbott

SEPTEMBER 1991

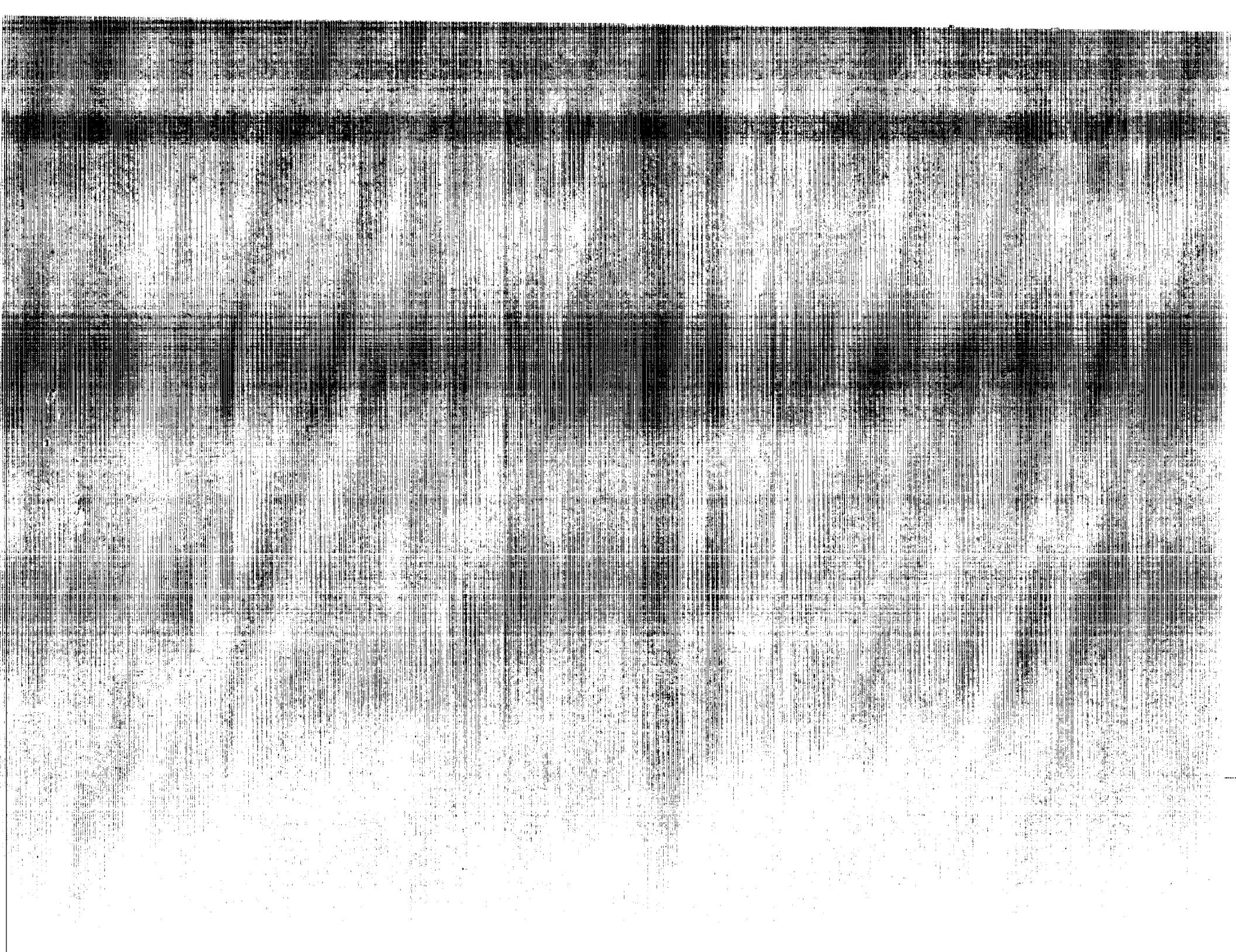

NASA Technical Memorandum 4285

A Compensatory Algorithm for the Slow-Down Effect on Constant-Time-Separation Approaches

Terence S. Abbott
Langley Research Center
Hampton, Virginia

National Aeronautics and
Space Administration
Office of Management
Scientific and Technical
Information Program
1991

Abstract

In seeking methods to improve airport capacity, the question arose as to whether an electronic display could provide information enabling the pilot to be responsible for self-separation under instrument conditions to allow for the practical implementation of reduced-separation, multiple glide-path approaches. This study involved the development and simulator validation of a time-based, closed-loop algorithm for in-trail approach and landing. This algorithm was designed to diminish the effects of approach speed reduction prior to landing for the trailing aircraft as well as the dispersion of the interarrival times. The operational task for the validation was an instrument approach to landing while following a single lead aircraft on the same approach path. The desired landing separation was 60 sec. An open-loop algorithm was the basis for comparison. The results of this study showed that relative to the open-loop algorithm, the closed-loop algorithm could theoretically provide for a 6-percent increase in runway throughput. From these results, it is concluded that by using a time-based, closed-loop spacing algorithm, precise interarrival time intervals may be achievable with operationally acceptable pilot workload.

Introduction

In general, airports operate at a higher efficiency during visual flight conditions than during instrument meteorological conditions. Two primary airborne techniques that, in conjunction, may allow airports operating under instrument conditions to achieve nearly the same level of capacity as that realized under visual conditions are (1) multiple glide-path approach methods and (2) the reduction of the instrument flight rules interarrival separation intervals currently required between aircraft. Aircraft interarrival separation is presently dictated by runway occupancy time and wake-vortex considerations (through vortex-dissipation times). The multiple glide-path approach method offers the potential to reduce interarrival separation through the avoidance of wake vortices, rather than through their dissipation. By providing the trailing aircraft with either a higher or laterally offset (upwind or closely spaced parallel runway) approach path, reduced-separation approaches may be possible with minimum vortex hazard.

In seeking methods to improve airport capacity, therefore, the question arose as to whether an electronic display, presenting the data-linked position of surrounding aircraft traffic, could provide information which would enable the pilot to be responsible for self-separation under instrument conditions to allow for the practical implementation of reduced-separation, multiple glide-path approaches. Two research studies have been completed (refs. 1 and 2) which address this question. These studies have shown that an increase of situational awareness, relative to conventional instrument flight, was provided by the displayed traffic information. They also showed that multiple glide-slope approaches, procedurally designed for vortex avoidance, are possible which maintain pilot workload and performance within operationally acceptable limits. It is noteworthy that these results were obtained with planned, in-trail aircraft separation times or interarrival times (IAT) as small as 45 sec.

In maximizing runway capacity, reducing the IAT is obviously a primary consideration. Additionally, two other IAT-related factors influence runway capacity. The first factor is the difference between the projected and the actual IAT. That is, the lead aircraft and the trailing aircraft may be perfectly separated as the lead aircraft lands, but due to approach speed reduction prior to landing for the trailing aircraft, the actual IAT is greater than the projected. From the studies of references 1 and 2, this added approximately 8 sec to an actual threshold crossing time of approximately 98 sec for a projected 90-sec IAT (both controller and self-spacing) and added approximately 3 sec for the 60-sec and 45-sec separation cases.

The second factor affecting runway capacity is the IAT dispersion. That is, the less that the IAT varies from the mean IAT, the shorter the mean IAT can be for an equivalent level of missed approaches (ref. 3). Figure 1 illustrates this effect of the IAT dispersion on runway arrival capacity. This effect is noteworthy since a secondary result of the first study (ref. 1) showed that a reduction of IAT dispersion relative to a controller providing separation cues is possible by using the displayed information for self-separation. (Controller separation was not used in the study of reference 2.) These interarrival time dispersions resulted in an average standard deviation of 4.9 sec for the controller-based separation and 1.9 sec for the self-separation cases.

In examining these two factors, it becomes obvious that the primary cause for both the slow-down effect and the IAT dispersion was that no spacing guidance was provided after the lead aircraft landed. From a controls viewpoint, the trailing aircraft at this point became open-looped. In order to reduce the effects of these two factors, the development and simulator validation of a time-based, closed-loop spacing algorithm was undertaken. This development and simulator validation is the topic of this paper.

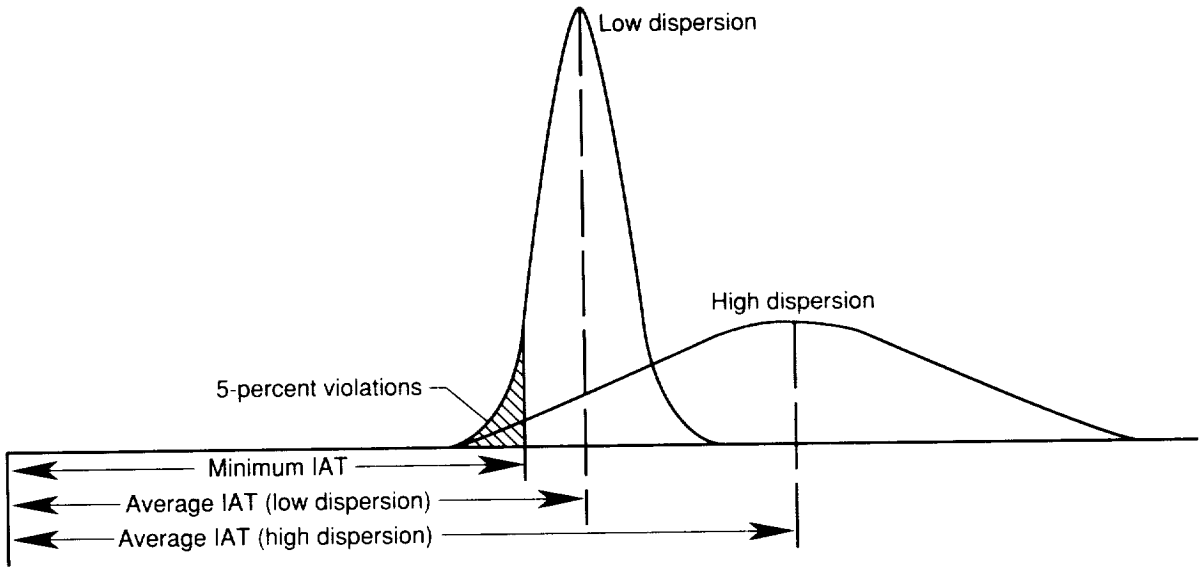

Figure 1. Effect of IAT dispersion on runway arrival capacity.

The time-based, closed-loop spacing algorithm and the associated cockpit display are a modification of the display and spacing algorithms developed during the studies of references 1 and 2. The information was presented on a forward-looking, head-up display (HUD) format that would permit the pilot to monitor and maintain a prespecified in-trail separation interval. The operational task for the simulation validation was an instrument landing system (ILS) approach to landing while following a single lead aircraft on the same approach path. The desired landing separation was 60 sec for these approaches. For the validation, each of three pilots flew six approaches with data being taken primarily in the form of quantitative measurements.

Symbols and Abbreviations

AGS	aircraft-guidance symbol
G_1, G_2, G_3	mathematical gains
HUD	head-up display
IAS	indicated airspeed, knots
IAT	interarrival time
ILS	instrument landing system
K	mathematical constant
L_{past}	past position of lead aircraft
L_{present}	present position of lead aircraft
R_F	range of following aircraft to runway, ft
$R_{F,\text{ref}}$	approximate point where following aircraft reaches $V_{F,\text{ref}}$, ft
$R_{F,o}$	range of following aircraft to runway when $R_L = 0$, ft
R_L	range of lead aircraft to runway, ft
$R_{L,\text{ref}}$	approximate point where lead aircraft reaches $V_{L,\text{ref}}$, ft
R_X	assumed maximum range of lead aircraft
S	ground speed, ft/sec
SDC	slow-down compensator
standard	standard spacing algorithm
T_{cross}	time since lead aircraft crossed runway threshold, sec
T_{des}	desired separation time, sec
$T_{\text{err},1}$, $T_{\text{err},2}$	time error terms, sec
T_F	estimated time of following aircraft to go from R_L to runway, sec
$T_{F,\text{in}}$	estimated time of following aircraft to go from R_F to $R_{F,\text{ref}}$, sec
$T_{F,\text{out}}$	estimated time of following aircraft to go from $R_{F,\text{ref}}$ to runway, sec

T_L	estimated time of lead aircraft to go from R_L to runway, sec
$T_{L,\text{in}}$	estimated time of lead aircraft to go from R_L to $R_{L,\text{ref}}$, sec
$T_{L,\text{out}}$	estimated time of lead aircraft to go from $R_{L,\text{ref}}$ to runway, sec
T_{land}	estimated time of following aircraft to landing, sec
T_{nom}	nominal time separation, sec
V_{err}	ground speed error, ft/sec
V_F	ground speed of following aircraft, ft/sec
$V_{F,\text{ref}}$	final approach ground speed of following aircraft, ft/sec
$V_{F,\text{req}}$	V_F required to achieve proper separation
V_L	ground speed of lead aircraft, ft/sec
VLDS	visual landing display system
$V_{L,\text{ref}}$	final approach ground speed of lead aircraft, ft/sec
V_{ref}	reference final approach speed as indicated airspeed, knots
ΔR	range between lead aircraft and following aircraft, ft
ΔT_{nom}	deviation from nominal time separation, sec

Research System

Simulator Description

This study employed the Langley Visual/Motion Simulator, which is a part-task, six-degree-of-freedom, motion-base simulator capable of presenting acceleration and attitude cues to the pilot. Audio cues for aerodynamic buffeting and engine noise were also provided. The aircraft dynamics modeled were those of a Boeing 737 and included nonlinear aerodynamic data and atmospheric effects. Conventional electromechanical navigation instruments, which included a horizontal-situation indicator, a flight director, and distance-measuring equipment (DME), were provided in the cockpit. Neither an autopilot nor a stability augmentation system was provided for the pilot. In addition, no attempt was made to duplicate any specific aircraft cockpit configuration or control-wheel force-feel characteristics. This simulator is further described in reference 4.

Additions to the aircraft force and moment equations caused by the vortex flow fields were made based on a strip-theory technique described in reference 5. The vortices generated by this method were for a lead aircraft that approximated the normal landing configuration of a Boeing 747 (wing leading- and trailing-edge flaps deployed, all landing flaps at 30°, landing gear down, a lift coefficient of 1.40, and a velocity of 140 knots) at a weight of 509 914 lb. After generation, the vortices descended at a rate of 6 ft/sec until they reached a point 600 ft below their generation point, at which time they ceased to descend. To simulate ground effect, vortices that came within 60 ft of the ground were held at that altitude and were spread outward at a rate of 6 ft/sec. The lower than nominal descent rate of the vortices (with nominal being approximately 7 to 8 ft/sec) and the lower than nominal maximum descent position (with nominal being approximately 900 ft below the generation point) were used to provide worse than normal vortex conditions by keeping the vortices closer to the flight path of the generating aircraft.

The visual landing display system (VLDS) provided the pilot with an out-the-window color scene of the simulated terrain. The system used a 60-ft by 24-ft three-dimensionally scaled terrain model, including a large commercial airport, that was traversed in three axes by a gantry carrying a closed-circuit color television camera. Gantry movements accounted for the aircraft spatial position, whereas the television-probe optics-system motions accounted for the heading, pitch, and bank of the aircraft. Additionally, the capability existed to simulate instrument meteorological conditions flight with this system by the employment of a controllable skyplate in its optical probe. Camera and gantry motions were commanded by the aircraft-simulation computer program, and the resulting scene was routed to the window screen of the simulator.

Primary Display Hardware

The primary pilot display for this study employed an out-the-window virtual image system of the beam-splitter, reflective-mirror type. The system, located nominally 50 in. from the pilot's eyes, presented a nominal 48° width by 36° height field of view of a 525-line raster video system and provided a 46° by 26° instantaneous field of view. The system supplies a color picture of unity magnification with a resolution on the order of 9 min of arc (ref. 4). The forward-looking, HUD-type presentation for this

study was obtained by mixing the video signal from the VLDS camera with the video output from an Adage AGT 340 graphics system, which generated the HUD symbology. The HUD display format was software windowed to provide a 30° wide by 20° high field of view.

Traffic Generation Technique

The displayed traffic was generated from data previously recorded by using the Langley Flight Simulation Computing Subsystems. Specifically, the traffic data were created by using a piloted simulation capability, wherein flights were made along a path that was prescribed by the test scenario. The data from these individual flights were recorded and then, by time correlation, were used as the parameters for the lead aircraft. For this study, two landing speeds for the lead aircraft were used—120 and 140 knots—to represent landing speeds of large and heavy aircraft.

Experimental Design

Basic-Display Format

The display format on which the traffic information was added was the ILS approach portion of the HUD format developed for the McDonnell Douglas DC-9-80, now known as the MD-80 (refs. 6 to 8). Information on this display was made available by the Douglas Aircraft Company, who developed the concept, and Sundstrand Data Control, Inc., who designed and built the HUD equipment. This format was essentially command oriented in that of the three guidance-related symbols (command reference, aircraft guidance, and category II ILS "window"), only the command-reference symbol moved conformally with the external view. The components of this format, shown in figure 2 for an arbitrary situation, were as follows: The attitude reference marker, which was a nonmoving symbol, was used in conjunction with the horizon line to indicate pitch attitude and heading. The horizon line and the associated pitch scales moved conformally with the pitch and roll attitudes of the aircraft. Additionally, these scales translated in the roll axis to indicate the drift-correction angle ("crab" angle) of the aircraft. This angle was determined by comparing the course reference symbol, which was fixed to the horizon line, with the heading symbol, which moved in pitch and roll with the horizon line but did not translate with heading. The command-reference symbol was always aligned under the course-reference symbol and overlaid the aiming point on the runway. The aircraft-guidance symbol (AGS) can be thought of as the position projection of the aircraft being flown. The movement of

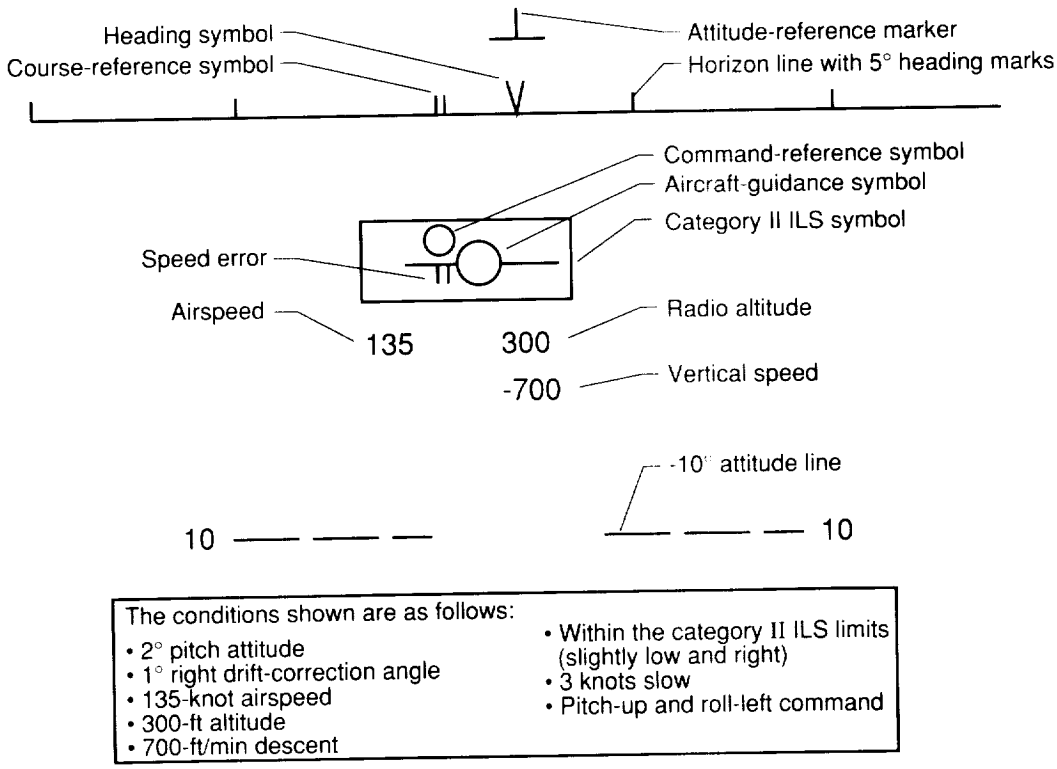

Figure 2. Basic-display format.

this symbol (which combined the desired glide-slope angle, the ILS error, and various aircraft position and attitude parameters) was such that by overlaying the command-reference symbol with this symbol, a smooth transition to the glide path could occur and be maintained. The category II ILS window symbol provided a measure of deviation from the nominal glide path and was referenced to the AGS; however, the scaling was not unity and the location of the window symbol was not conformal with the outside view unless the aircraft was flying exactly along the nominal approach path.

It should be noted that the guidance symbology was designed for category II ILS approaches. In addition to these attitude- and path-guidance symbols, a speed-error symbol was also provided. This symbol grew vertically as a function of speed error where a 3-knots-fast indication would show the symbol being above the "wing" line of the AGS and its length equal to the radius of the center circle of the guidance symbol. The error signal to drive this symbol would normally come from the flight-director algorithm of the aircraft.

Traffic-Display

The basic traffic-display (fig. 3), developed in references 1 and 2, was a modification of the basic-display format with the addition of three symbols: the present-position symbol of the lead aircraft, the past-position symbol of the lead aircraft, and the numeric symbol for deviation from nominal time spacing. The general concept in the formulation of these symbols was to provide the pilot with adequate information so that he could (1) assess the potential danger stemming from the vortices generated by the lead aircraft, (2) modify his approach profile for vortex avoidance, and (3) adjust his speed to provide for adequate in-trail separation. With this in mind, it was determined that the lateral deviation of the lead aircraft relative to the glide path was of no concern to the follower as long as the lead aircraft remained within nominal ILS limits. For this reason, and while the within-limits condition was met, the lateral position of the lead aircraft was not shown to the follower. The rationale and implementation for each of the symbols are provided below (along with a section describing the standard spacing algorithm).

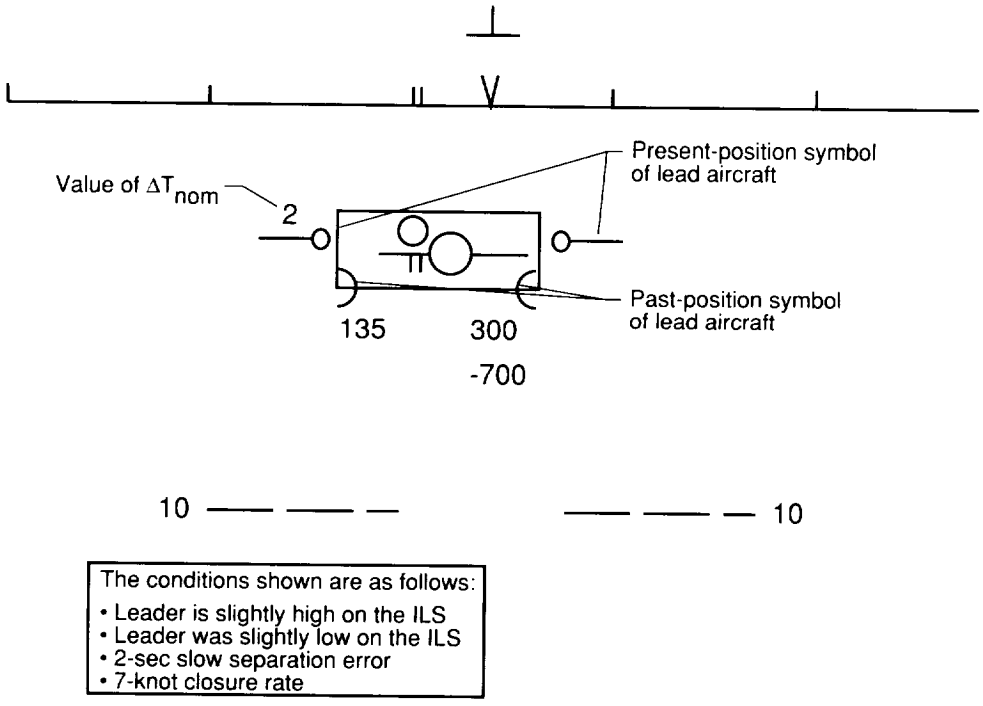

Figure 3. Traffic-display format.

Present-position symbol of lead aircraft. The primary purpose of the present-position symbol of the lead aircraft (L_{present}), which was represented by a left and right "wing," was to provide information to the pilot on how accurately the lead aircraft was following the intended path. This symbol was driven vertically as a function of the ILS glide-slope error of the lead aircraft in the same manner as the ILS box. The exception was that, unlike the basic display where the ILS box was driven relative to the AGS, the L_{present} symbol was driven relative to the ILS box. To prevent a misinterpretation of the flare maneuver as a missed approach maneuver, the vertical position was "frozen" once the lead aircraft descended below a 100-ft altitude.

Two lateral motions were also possible with the L_{present} symbol, and these, as well, were based relative to the ILS box. The first motion was a function of the closure rate on the lead aircraft, wherein each half of the symbol (the wings) moved either toward the other (indicating an increase in separation) or farther apart (indicating a decrease in separation). The motion was scaled such that a 20-knot closure rate would reflect as a gap, between the circular ends of the symbol and the ILS-box edge, equal to one-quarter of the width of the ILS box. This closure-rate indication was also limited to 20 knots. The second lateral motion that this symbol would exhibit was a function of the lateral ILS error of the lead aircraft and would occur only when the error was greater than approximately ½°. At this time, the symbol would move laterally as a function of ILS localizer error with the wing opposite the direction of motion being blanked to reduce display clutter. In other words, if the lead aircraft was deviating to the right, the right wing would move to the right and the left wing would be blanked. This feature was important during the last portion of the approach in that the pilot could tell whether or not the lead aircraft was exiting the runway.

Past-position symbol of lead aircraft. The primary purpose of the past-position symbol of the lead aircraft (L_{past}), which was represented by a left and a right half-circle, was to provide some general information as to where the vortices generated by the lead aircraft were relative to the following aircraft (referred to as ownship). The implementation of this symbol was simply a "playback" of the position of the stored L_{present} symbol relative to the ILS box. That is, if ownship was positioned 10 n.mi. from the runway, the L_{past} symbol indicated the position of the lead aircraft when it also was 10 n.mi. from the runway. Since vortices normally descend after generation, the top of each half-circle of the L_{past} symbol was placed on the display at the position that was previously occupied by the circular ends of the wings of the L_{present} symbol. This implied a descending condition. Unlike the L_{present} symbol that "froze" when the lead aircraft descended below 100 ft in altitude, the L_{past} symbol remained active until ownship landed.

Standard Spacing Algorithm

The deviation from nominal time spacing (ΔT_{nom}) term was the primary variable for determining and adjusting the in-trail separation. The numeric value denoting ΔT_{nom} was designed to aid the pilot in maintaining the prescribed in-trail separation and was an indication, in seconds, of the separation error. The information presented by this symbol was based on the desired separation time (T_{des}), the estimated time that it would take the lead aircraft to reach the runway threshold (R_L/V_L), and an adjustment term to compensate for the differences in assumed final approach speeds between the lead aircraft and ownship ($V_{L,\text{ref}}/V_{F,\text{ref}}$). This value was not displayed after the lead aircraft crossed the runway threshold.

In addition to the numeric display of ΔT_{nom}, shown over the left side of the AGS, a numeric display of ΔR, displayed in tenths of nautical miles, was shown over the right side of the AGS at any time that ΔR became less than 12 152 ft or 2 n.mi.

One additional modification was implemented in the traffic display in an attempt to reduce pilot workload due to the in-trail separation task. This modification involved driving the speed-error symbol on the basic format with a speed-error term that was a function of the speed of ownship, the in-trail separation, and ΔT_{nom}. This modification was used prior to the lead aircraft crossing the runway threshold. After the lead aircraft crossed the threshold, the basic-format speed-error term was used. A detailed description of this algorithm is given in appendix A.

Compensatory Spacing Algorithm

To compensate for the slow-down effect, as well as to reduce IAT dispersion, a closed-loop spacing algorithm was developed. This algorithm, termed the slow-down compensator (SDC), was a modification of the algorithm of the basic traffic-display. The time-spacing algorithm used in the basic traffic-display, as with other constant-time spacing schemes (to include constant time delay), was designed to provide for a nominal separation as the lead aircraft crosses the runway threshold.

If ownship was not at the final approach speed as the lead aircraft crossed the threshold, the approach

profile would be as shown in figure 4 (assuming that ownship was initially faster than the final approach speed). For the actual time difference between the lead aircraft and the trailing aircraft to be equal to T_{des}, the trailing aircraft would have to maintain the ground speed it had at $R_L = 0$ (assuming also that $\Delta T_{\text{nom}} = 0$ at that time). Since in a "real world" application this case would in most respects be unacceptable from an operational and safety standpoint, an algorithm was developed to compensate for the slow-down effect through a continuous adjustment of T_{nom}. The algorithm was divided into two parts; one part for $R_L > 0$ and the other part for $R_L \leq 0$.

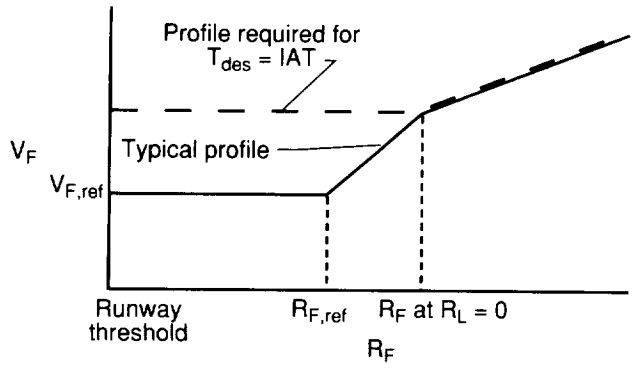

Figure 4. Speed versus range, utilizing a constant time separation algorithm.

$R_L > 0$. For the IAT to equal T_{des}, the time for ownship to reach the runway (T_F) must be equal to the time for the lead aircraft to reach the runway (T_L) plus T_{des}. To determine the time required for the lead aircraft to reach the runway threshold, two calculations must be made. The first of these determines the estimated time required for the lead aircraft to reach the runway threshold from the point where it would reach final approach speed. The second calculation determines the estimated time required for the lead aircraft to reach final approach speed (assuming that the lead aircraft is currently faster than the final approach speed) from its current position and speed. Similar calculations are then made for ownship. A ΔT_{nom} term was then determined in a manner similar to the standard separation algorithm. A modified speed-error was also provided, based on the new value of ΔT_{nom}.

$R_L \leq 0$. Once the lead aircraft crossed the runway threshold, the SDC algorithm was based on T_{nom}, where $T_{\text{nom}} = T_{\text{des}} - T_{\text{cross}}$, and T_{cross} equaled the time since the lead aircraft crossed the runway threshold. Speed-error, time-error, and ΔT_{nom} terms were then calculated as a function of T_{nom}. A detailed description of this algorithm is given in appendix B.

Task Description

The piloting task for the validation of this concept was a manual, instrument approach and landing while following the vortex-generating lead aircraft in weather conditions which simulated a 150-ft ceiling and calm air. The approach was to runway 26L at the Stapleton International Airport, Denver, Colorado. The test subjects were instructed to fly the simulator in a manner they deemed acceptable for airline operations and to avoid radical maneuvers. Besides being professional pilots, the test subjects had attended an airline training school and were experienced in flying Boeing aircraft. During the test runs, the test engineer acted as the copilot with regard to lowering the flaps and other such tasks as directed by the evaluation pilot.

During this study, the means for providing the in-trail separation was divided into two categories: standard and SDC. Under standard separation, the pilot used the basic traffic-display with the associated separation algorithm. Under SDC separation, the pilot used the traffic-display with the SDC algorithm. In both cases, the T_{des} value was set to 60 sec.

Traffic Profiles

The traffic scenario utilized in this validation was that of a single lead aircraft flying the ILS approach to runway 26L at the Stapleton International Airport. Two profiles for the lead aircraft were used and are described in the following discussion.

Profile 1. This traffic profile was that of an aircraft with a $V_{\text{ref}} = 120$ knots (the same as that of ownship). This aircraft flew an almost idle thrust descent while carefully maintaining the ILS path. It landed and exited the runway in a normal but expeditious manner. This profile was considered the baseline profile.

Profile 2. This traffic profile was used to evaluate the effect of dissimilar approach speeds. The approach speed simulated that of a heavier aircraft with $V_{\text{ref}} = 140$ knots. This aircraft carefully maintained the ILS path, landed, and exited the runway in a normal but expeditious manner.

Test Conditions

A total of 18 simulated instrument approaches were flown by 3 pilots to obtain data, each pilot flying 6 approaches. The test matrix for each pilot is shown in table I. Sufficient training was given prior to the initial simulation data sessions to minimize the

learning effects. The pilots were trained in all situations shown in the test matrix. The initial conditions for the lead aircraft were as follows: on the ILS path, at an IAS of 250 knots, and approximately 15 n.mi. from the runway threshold. The initial conditions for ownship were as follows: on the ILS path, at an IAS of 250 knots, and at a distance behind the lead aircraft such that ΔT_{nom} was approximately zero.

Table I. Text Matrix

Sequence number	Algorithm	Lead aircraft V_{ref}, knots
1	Standard	120
2	Standard	120
3	SDC	120
4	SDC	120
5	Standard	140
6	SDC	140

Results and Discussion

The primary results of the validation were the measurements of the actual IAT. These results are shown in tables II and III. The differences in both the IAT and the IAT dispersions between the two guidance algorithms were significant at the 5-percent level. The mean IAT for the standard algorithm was 63.26 sec (3.26 sec mean error relative to the desired 60-sec separation), and the mean IAT for the SDC algorithm was 59.96 sec (−0.04 sec mean error). The IAT standard deviation for the standard algorithm was 0.36 sec and the IAT standard deviation for the SDC algorithm was 0.09 sec. The differences between these standard deviation values, while statistically significant, were not operationally meaningful. However, the differences in the mean IAT were operationally significant in that the SDC can theoretically provide for a 6-percent increase in runway throughput.

Path-tracking performance (ILS glide-slope and localizer error) was also analyzed. Relative to the guidance algorithm used, no differences in either lateral or vertical tracking performance were noted.

Pilot comments indicated that all three pilots felt the SDC guidance would be acceptable from an operational standpoint. Two of the pilots noted that they could not detect any major difference between the algorithms with respect to their workload. Additionally, all commented that the mechanization of the speed-error term using the speed-error symbol on the display was very similar to the fast-slow indicator on a conventional attitude-director indicator (ADI). Because of this, it was very easy to use.

Table II. IAT

Guidance	Lead aircraft V_{ref}, knots	IAT, sec		
		Pilot 1	Pilot 2	Pilot 3
Standard	120	63.35	63.39	63.97
Standard	120	63.20	62.78	63.03
Standard	140	62.96	63.09	63.56
SDC	120	60.01	59.90	59.98
SDC	120	59.82	59.85	60.04
SDC	140	60.01	59.95	60.09

Table III. IAT Error

Guidance	Lead aircraft V_{ref}, knots	IAT error, sec		
		Pilot 1	Pilot 2	Pilot 3
Standard	120	+3.35	+3.39	+3.97
Standard	120	+3.20	+2.78	+3.03
Standard	140	+2.96	+3.09	+3.56
SDC	120	+0.01	−0.10	−0.02
SDC	120	−0.18	−0.15	+0.04
SDC	140	+0.01	−0.05	+0.09

Conclusions

This study involved the development and simulator validation of a time-based, closed-loop algorithm for in-trail (one aircraft behind the other) approach and landing. This algorithm was designed to reduce the effects of approach speed reduction prior to landing for the trailing aircraft as well as to reduce the interarrival time (IAT) dispersion. The operational task for the validation was an instrument approach to landing while following a single lead aircraft on the same approach path. The desired landing separation was 60 sec for these approaches. An open-loop algorithm, developed in previous work, was used as the basis for comparison. For this validation, each of three pilots flew six approaches with data being taken primarily in the form of quantitative measurements. From these results, the following conclusions were drawn:

1. For the desired IAT of 60 sec, the use of the open-loop algorithm resulted in a 3.26-sec mean error, while the closed-loop algorithm resulted in a −0.04-sec mean error. The IAT deviation with either algorithm was less than 0.5 sec.

2. Relative to the open-loop algorithm, the closed-loop algorithm could theoretically provide for a 6-percent increase in runway throughput.
3. The use of the closed-loop algorithm did not affect the path-tracking performance.
4. Pilot comments indicated that the guidance from the closed-loop algorithm would be acceptable from an operational standpoint.

From these results, it is concluded that by using a time-based, closed-loop spacing algorithm, precise IAT intervals may be achievable with operationally acceptable pilot workload.

NASA Langley Research Center
Hampton, VA 23665-5225
July 22, 1991

NASA
National Aeronautics and Space Administration

Report Documentation Page

1. Report No.	2. Government Accession No.	3. Recipient's Catalog No.
NASA TM-4285		

4. Title and Subtitle	5. Report Date
A Compensatory Algorithm for the Slow-Down Effect on Constant-Time-Separation Approaches	September 1991
	6. Performing Organization Code
7. Author(s)	8. Performing Organization Report No.
Terence S. Abbott	L-16922
9. Performing Organization Name and Address	10. Work Unit No.
NASA Langley Research Center Hampton, VA 23665-5225	505-64-13
	11. Contract or Grant No.
12. Sponsoring Agency Name and Address	13. Type of Report and Period Covered
National Aeronautics and Space Administration Washington, DC 20546-0001	Technical Memorandum
	14. Sponsoring Agency Code

15. Supplementary Notes

16. Abstract

In seeking methods to improve airport capacity, the question arose as to whether an electronic display could provide information enabling the pilot to be responsible for self-separation under instrument conditions to allow for the practical implementation of reduced-separation, multiple glide-path approaches. This study involved the development and simulator validation of a time-based, closed-loop algorithm for in-trail approach and landing. This algorithm was designed to diminish the effects of approach speed reduction prior to landing for the trailing aircraft as well as the dispersion of the interarrival times. The operational task for the validation was an instrument approach to landing while following a single lead aircraft on the same approach path. The desired landing separation was 60 sec. An open-loop algorithm was the basis for comparison. The results of this study showed that relative to the open-loop algorithm, the closed-loop algorithm could theoretically provide for a 6-percent increase in runway throughput. From these results, it is concluded that by using a time-based, closed-loop spacing algorithm, precise interarrival time intervals may be achievable with operationally acceptable pilot workload.

17. Key Words (Suggested by Author(s))	18. Distribution Statement
Cockpit display	Unclassified - Unlimited Subject Category 06

19. Security Classif. (of this report)	20. Security Classif. (of this page)	21. No. of Pages	22. Price
Unclassified	Unclassified	17	A03

NASA FORM 1626 OCT 86

NASA-Langley, 1991

For sale by the National Technical Information Service, Springfield, Virginia 22161-2171

2. Relative to the open-loop algorithm, the closed-loop algorithm could theoretically provide for a 6-percent increase in runway throughput.

3. The use of the closed-loop algorithm did not affect the path-tracking performance.

4. Pilot comments indicated that the guidance from the closed-loop algorithm would be acceptable from an operational standpoint.

From these results, it is concluded that by using a time-based, closed-loop spacing algorithm, precise IAT intervals may be achievable with operationally acceptable pilot workload.

NASA Langley Research Center
Hampton, VA 23665-5225
July 22, 1991

Appendix A

Standard Spacing Algorithm

The number denoting a deviation from nominal time spacing (ΔT_{nom}) was designed to aid the pilot in maintaining the in-trail separation and was an indication, in seconds, of his separation error. The symbol ΔT_{nom} is defined as

$$\Delta T_{\text{nom}} = \frac{(\Delta R - T_{\text{nom}} V_F)}{V_{F,\text{ref}}} \tag{1}$$

where ΔR is the in-trail separation, V_F is the current ground speed of ownship, $V_{F,\text{ref}}$ is the nominal final approach speed (V_{ref}) of ownship (the final speed that ownship should decelerate to, which is a value selected before the approach begins), and T_{nom} is defined as

$$T_{\text{nom}} = T_{\text{des}} + \frac{R_L}{V_L}\left(1 - \frac{V_{L,\text{ref}}}{V_F, \text{ref}}\right)$$

where R_L is the current range to the runway of the lead aircraft, V_L is the current ground speed of the lead aircraft, T_{des} is the desired (and preselected) separation time as the lead aircraft crosses the runway threshold, and $V_{L,\text{ref}}$ is the assumed nominal approach speed of the lead aircraft. The $\frac{R_L}{V_L}\left(1 - \frac{V_{L,\text{ref}}}{V_{F,\text{ref}}}\right)$ term is used to compensate for dissimilar approach speeds. Any error generated from a miscalculation in nominal approach speeds, which are usually based on aircraft type, will diminish as the lead aircraft approaches the runway.

In addition to the numeric display of ΔT_{nom}, which was shown over the left side of the AGS, a numeric display of ΔR, displayed in tenths of nautical miles, was shown over the right side of the AGS any time that ΔR became less than 2 n.mi. It should be noted that most of the concepts for the traffic display, noted previously, were obtained under a contract to Dynasyst, Inc., of Princeton, New Jersey.

One additional modification was implemented in the traffic display in an attempt to reduce pilot workload due to the in-trail separation task. This modification involved driving the speed-error symbol on the basic format with a speed-error term obtained from equation (1). A zero ΔT_{nom} is the quantity actually desired. Therefore, set ΔT_{nom} equal to zero in equation (1) and solve for V_F, which is actually, then, the required V_F (that is, $V_{F,\text{req}}$) for ΔT_{nom} equal to zero. Thus

$$\frac{(\Delta R - T_{\text{nom}} V_{F,\text{req}})}{V_{F,\text{ref}}} = 0$$

Solving for $V_{F,\text{req}}$

$$V_{F,\text{req}} = \frac{\Delta R}{T_{\text{nom}}} \tag{2}$$

Thus, speed error is

$$\text{Speed error} = V_F - V_{F,\text{req}} \tag{3}$$

The $V_{F,\text{req}}$ term returned to the nominal approach speed for the aircraft after the lead aircraft crossed the runway threshold.

Appendix B

Compensatory Spacing Algorithm

To compensate for the slow-down effect as well as to reduce IAT dispersion, a closed-loop spacing algorithm was developed. This algorithm, termed the slow-down compensator (SDC), was a modification of the standard algorithm of the basic traffic-display. The time-spacing algorithm used in the basic traffic-display, as with other constant-time spacing schemes (including constant-time delay), was designed to provide the nominal separation as the lead aircraft crosses the runway threshold.

If ownship was not at the final approach speed as the lead aircraft crossed the threshold, the approach profile would typically cause the actual IAT to be greater than T_{des}. For the actual time difference between the lead aircraft and the trailing aircraft to be equal to T_{des}, the ownship would have to maintain the ground speed it had when $R_L = 0$ (assuming also that $\Delta T_{\text{nom}} = 0$ at that time). Since, in a "real world" application this case would in most respects be unacceptable from an operational and safety standpoint, an algorithm was developed to compensate for the slow-down effect by the continuous adjustment of T_{nom}. The algorithm was divided into two parts: one part for $R_L > 0$ and the other part for $R_L \leq 0$. A flowchart of the algorithm is given in figure B1 and a narrative description is given below.

$R_L > 0$

For the IAT to equal T_{des}, the time for ownship to reach the runway must equal the time for the lead aircraft to reach the runway plus T_{des}. That is,

$$T_{F,\text{in}} + T_{F,\text{out}} = T_L + T_{\text{des}} \tag{1}$$

where $T_{F,\text{in}}$ is the time required for ownship to fly from the point $R_{F,\text{ref}}$ (approximate point where ownship reaches $V_{F,\text{ref}}$) to the runway threshold, $T_{F,\text{out}}$ is the time required to go from R_F to $R_{F,\text{ref}}$ (assuming a linear deceleration), and T_L is the time required for the lead aircraft to fly from R_L to the runway threshold. To determine the time required for ownship to reach the runway, let

$$T_{F,\text{in}} = \frac{R_{F,\text{ref}}}{V_{F,\text{ref}}}$$

and let

$$T_{F,\text{out}} = \frac{R_F - R_{F,\text{ref}}}{(V_F + V_{F,\text{ref}})/2} \tag{2}$$

Two equations, similar to $T_{F,\text{in}}$ and $T_{F,\text{out}}$, are derived for the lead aircraft. Let

$$T_{L,\text{in}} = \frac{R_{L,\text{ref}}}{V_{L,\text{ref}}} \tag{3}$$

where $T_{L,\text{in}}$ is the time required for the lead aircraft to fly from the point $R_{L,\text{ref}}$ (the estimated point where the lead aircraft reaches $V_{L,\text{ref}}$) to the runway threshold. Let

$$T_{L,\text{out}} = \frac{R_L - R_{L,\text{ref}}}{(V_L + V_{L,\text{ref}})/2} \tag{4}$$

where $T_{L,\text{out}}$ is the time required to go from R_L to $R_{L,\text{ref}}$ (again assuming a linear deceleration). A generalized term T_L for the estimated time required for the lead aircraft to reach the runway threshold for any R_L was derived from equations (3) and (4):

$$T_L = G_1(T_{L,\text{in}} + T_{L,\text{out}}) + (1 - G_1)\frac{R_L}{V_L}$$

where

$$G_1 = 1 \qquad (R_L \geq R_{L,\text{ref}})$$

$$G_1 = \frac{R_L}{R_{L,\text{ref}}} \qquad (R_L < R_{L,\text{ref}})$$

The required V_F ($V_{F,\text{req}}$) to obtain IAT = T_{des} is (rearranging eq. (1))

$$T_{F,\text{out}} = T_L + T_{\text{des}} - T_{F,\text{in}}$$

Substituting equation (2) for $T_{F,\text{out}}$,

$$\frac{R_F - R_{F,\text{ref}}}{(V_{F,\text{req}} + V_{F,\text{ref}})/2} = T_L + T_{\text{des}} - T_{F,\text{in}}$$

then,

$$V_{F,\text{req}} = \frac{2(R_F - R_{F,\text{ref}})}{T_L + T_{\text{des}} - T_{F,\text{in}}} - V_{F,\text{ref}} \tag{5}$$

If $V_{F,\text{req}}$ from equation (5) is greater than the initial speed of ownship, then $V_{F,\text{req}}$ is set equal to the initial speed of ownship. This is to prevent an initial speed increase during the approach. Then T_{nom} and ΔT_{nom} are determined with a new T_{nom} (from eq. (2) of appendix A) corresponding to

$$T_{\text{nom}} = \frac{\Delta R}{V_{F,\text{req}}}$$

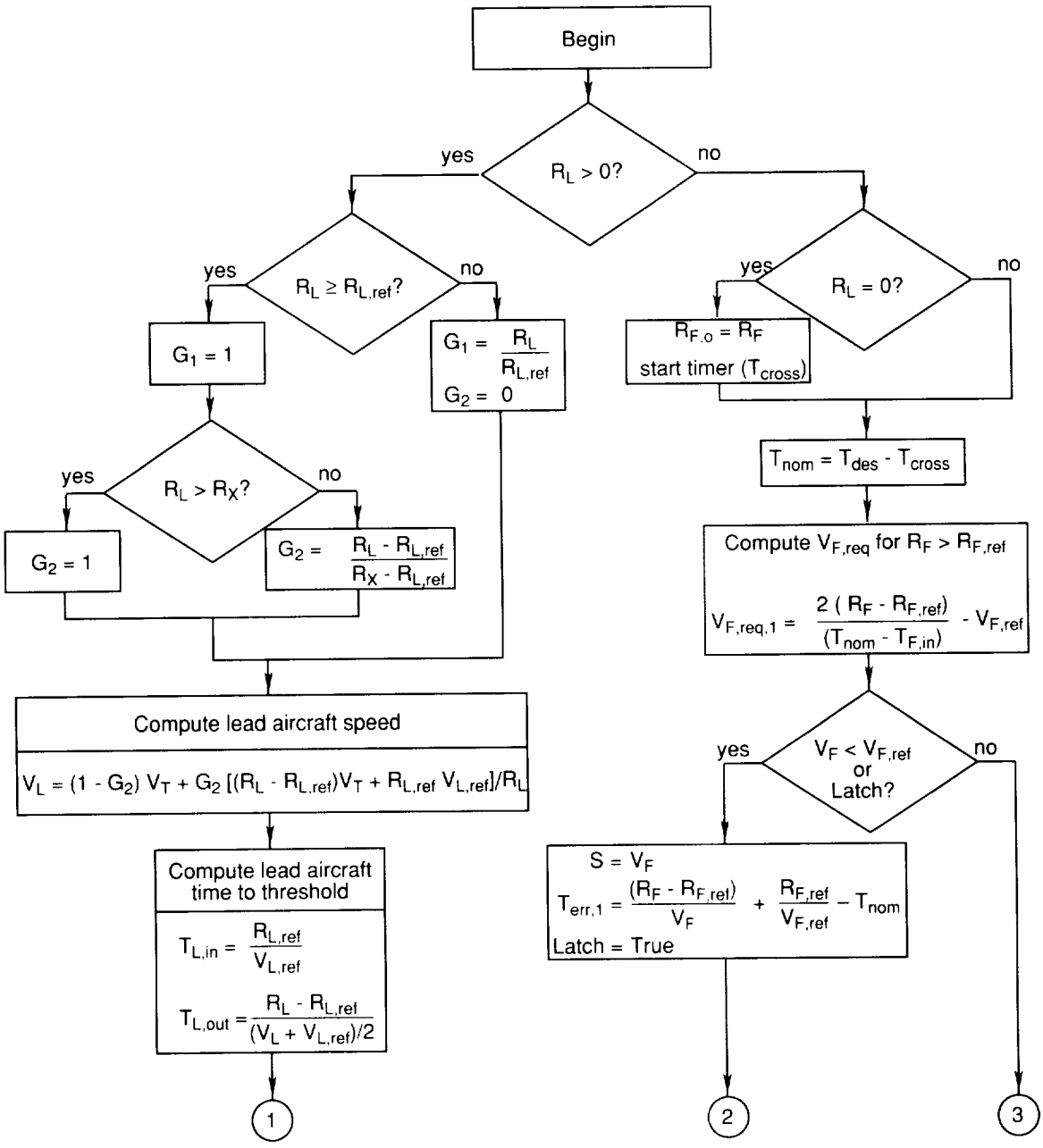

Figure B1. SDC algorithm flowchart.

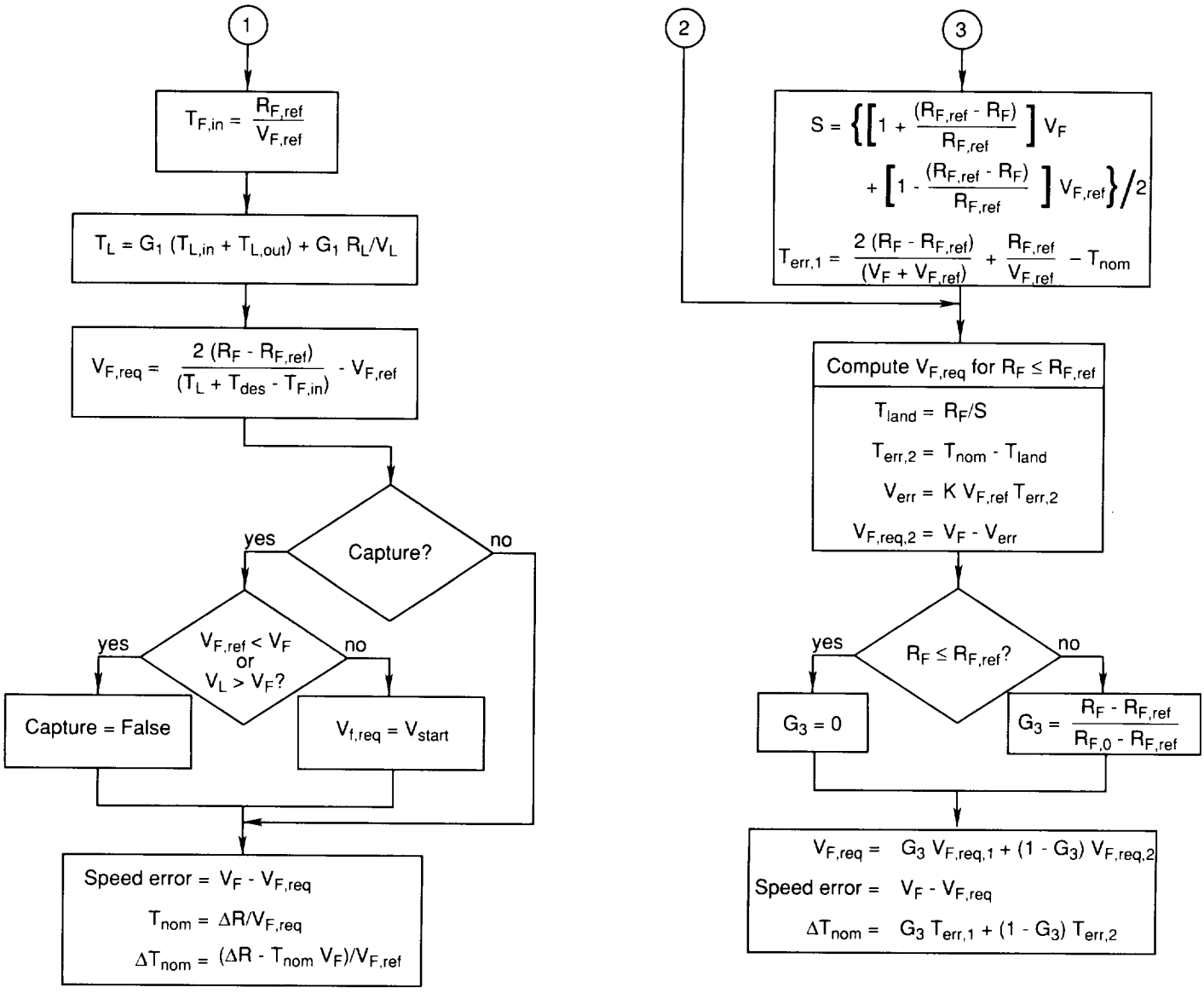

Inputs	Outputs	Initial conditions
R_L	Speed error	$R_{F,ref} = 0.8 V_{F,ref} T_{des}$
V_L	T_{nom}	$R_{L,ref} = 2.5$ n.mi.
R_F	ΔT_{nom}	$R_X = 20.0$ n.mi.
V_F		$V_{start} = V_F$
$V_{F,ref}$ (pilot selectable)		Capture = True
$V_{L,ref}$ (pilot selectable)		Latch = False
T_{des} (pilot selectable)		

Figure B1. Concluded.

with ΔT_{nom} computed as in equation (1) of appendix A. The speed-error term may then be computed using equation (3) of appendix A. It should be noted that the V_L term used in the SDC algorithm was

$$V_L = (1 - G_2)V_T + G_2 \left[V_T \frac{(R_L - R_{L,\text{ref}})}{R_L} + V_{L,\text{ref}} \frac{R_{L,\text{ref}}}{R_L} \right]$$

where V_T is the ground speed of the lead aircraft after passing through a first-order filter with $\tau = 10$ sec and

$$G_2 = 1 \qquad (R_L > R_X)$$

$$G_2 = \frac{(R_L - R_{L,\text{ref}})}{(R_X - R_{L,\text{ref}})} \qquad (R_{L,\text{ref}} < R_L < R_X)$$

$$G_2 = 0 \qquad (R_L < R_{L,\text{ref}})$$

where

$$R_X = 121\,520 \text{ ft (20 n.mi.)}$$

This derivation of V_L was used to provide a smooth (no discrete transitions) estimate of the speed profile of the lead aircraft for the three segments of the approach profile: $R_L > R_X$, $R_X > R_L > R_{L,\text{ref}}$, and $R_{L,\text{ref}} > R_L$.

$R_L \leq 0$

Once the lead aircraft crosses the runway threshold, the SDC algorithm is based on T_{nom} where

$$T_{\text{nom}} = T_{\text{des}} - T_{\text{cross}}$$

and T_{cross} is the time since $R_L \leq 0$. To determine the required speed, two computations are used: one for $R_F > R_{F,\text{ref}}$ and the other for $R_F \leq R_{F,\text{ref}}$. For $R_F > R_{F,\text{ref}}$, equation (5) may be used, substituting T_{nom} for T_{des} and setting T_L to zero, where

$$T_L = T_{L,\text{in}} + T_{L,\text{out}}$$

That is,

$$V_{F,\text{req}} = \frac{2(R_F - R_{F,\text{ref}})}{T_{\text{nom}} - T_{F,\text{in}}} - V_{F,\text{req}} \qquad (6)$$

For $R_F \leq R_{F,\text{ref}}$, the following derivation is used for $V_{F,\text{req}}$. Let

$$T_{\text{err},2} = T_{\text{nom}} - T_{\text{land}}$$

where

$$T_{\text{land}} = \frac{R_F}{S}$$

and

$$S = V_F \qquad (V_F < V_{F,\text{ref}})$$

otherwise

$$S = \left\{ \left[1 + \frac{(R_{F,\text{ref}} - R_F)}{R_{F,\text{ref}}} \right] V_F + \left[1 - \frac{(R_{F,\text{ref}} - R_F)}{R_{F,\text{ref}}} \right] V_{F,\text{ref}} \right\} /2$$

To determine $V_{F,\text{req}}$, let

$$V_{\text{err}} = K\, V_{F,\text{ref}}\, T_{\text{err},2}$$

where K is such that 1 sec of error is approximately equal to 5 knots ($K = 0.04$). Then,

$$V_{F,\text{req}} = V_F - V_{\text{err}} \qquad (7)$$

In order to preclude the possibility of a discontinuity at $R_F = R_{F,\text{ref}}$, the $V_{F,\text{req}}$ terms from equations (6) and (7) were combined to form a single $V_{F,\text{req}}$ term as follows: Let

$$V_{F,\text{req},1} = V_{F,\text{req}}$$

from equation (6) and

$$V_{F,\text{req},2} = V_{F,\text{req}}$$

from equation (7). Then let

$$V_{F,\text{req}} = G_3\, V_{F,\text{req},1} + (1 - G_3)\, V_{F,\text{req},2}$$

where

$$G_3 = 0 \qquad (R_F \leq R_{F,\text{ref}})$$

$$G_3 = \frac{(R_F - R_{F,\text{ref}})}{(R_{F,o} - R_{F,\text{ref}})} \qquad (R_F > R_{F,\text{ref}})$$

and where

$$R_{F,o} = R_F \qquad (R_L = 0)$$

Similarly,

$$\Delta T_{\text{nom}} = G_3\, T_{\text{err},1} + (1 - G_3)\, T_{\text{err},2}$$

where

$$T_{\text{err},1} = \frac{(R_F - R_{F,\text{ref}})}{V_F} + \frac{R_{F,\text{ref}}}{V_{F,\text{ref}}} - T_{\text{nom}} \qquad (V_F < V_{F,\text{ref}})$$

otherwise

$$T_{\text{err},1} = \frac{2(R_F - R_{F,\text{ref}})}{V_F + V_{F,\text{ref}}} + \frac{R_{F,\text{ref}}}{V_{F,\text{ref}}} - T_{\text{nom}}$$

References

1. Abbott, Terence S.: *Simulation of a Cockpit-Display Concept for Executing a Wake-Vortex Avoidance Procedure.* NASA TP-2300, 1984.

2. Abbott, Terence S.: *A Cockpit-Display Concept for Executing a Multiple Glide-Slope Approach for Wake-Vortex Avoidance.* NASA TP-2386, 1985.

3. Swedish, William J.: *Evaluation of the Potential for Reduced Longitudinal Spacing on Final Approach.* Rep. No. FAA-EM-79-7, Aug. 1979. (Available from DTIC as AD A076 434.)

4. Parrish, Russell V.; and Bowles, Roland L.: *Motion/Visual Cueing Requirements for Vortex Encounters During Simulated Transport Visual Approach and Landing.* NASA TP-2136, 1983.

5. Hastings, Earl C., Jr.; and Keyser, Gerald L., Jr.: *Simulator Study of Vortex Encounters by a Twin-Engine, Commercial, Jet Transport Airplane.* NASA TP-1966, 1982.

6. Lowe, J. R.: Improving the Accuracy of HUD Approaches in Windshear With a New Control Law. AIAA-78-1494, Aug. 1978.

7. Lowe, J. R.; and Ornelas, J. R.: Applications of Head-Up Displays in Commercial Transport Aircraft. *Collection of Technical Papers—AIAA 4th Digital Avionics Systems Conference*, Nov. 1981, pp. 409–414. (Available as AIAA-81-2300.)

8. *DC-9 Super 80 Flight Crew Operating Manual—Operating Procedures and Description.* McDonnell Douglas Corp., Dec. 1980, Section 4, 3-10-20, Code 1.

NASA
National Aeronautics and Space Administration

Report Documentation Page

1. Report No.	2. Government Accession No.	3. Recipient's Catalog No.
NASA TM-4285		

4. Title and Subtitle	5. Report Date
A Compensatory Algorithm for the Slow-Down Effect on Constant-Time-Separation Approaches	September 1991
	6. Performing Organization Code
7. Author(s)	8. Performing Organization Report No.
Terence S. Abbott	L-16922
9. Performing Organization Name and Address	10. Work Unit No.
NASA Langley Research Center Hampton, VA 23665-5225	505-64-13
	11. Contract or Grant No.
12. Sponsoring Agency Name and Address	13. Type of Report and Period Covered
National Aeronautics and Space Administration Washington, DC 20546-0001	Technical Memorandum
	14. Sponsoring Agency Code

15. Supplementary Notes

16. Abstract

In seeking methods to improve airport capacity, the question arose as to whether an electronic display could provide information enabling the pilot to be responsible for self-separation under instrument conditions to allow for the practical implementation of reduced-separation, multiple glide-path approaches. This study involved the development and simulator validation of a time-based, closed-loop algorithm for in-trail approach and landing. This algorithm was designed to diminish the effects of approach speed reduction prior to landing for the trailing aircraft as well as the dispersion of the interarrival times. The operational task for the validation was an instrument approach to landing while following a single lead aircraft on the same approach path. The desired landing separation was 60 sec. An open-loop algorithm was the basis for comparison. The results of this study showed that relative to the open-loop algorithm, the closed-loop algorithm could theoretically provide for a 6-percent increase in runway throughput. From these results, it is concluded that by using a time-based, closed-loop spacing algorithm, precise interarrival time intervals may be achievable with operationally acceptable pilot workload.

17. Key Words (Suggested by Author(s))	18. Distribution Statement
Cockpit display	Unclassified—Unlimited Subject Category 06

19. Security Classif. (of this report)	20. Security Classif. (of this page)	21. No. of Pages	22. Price
Unclassified	Unclassified	17	A03

NASA FORM 1626 OCT 86

NASA-Langley, 1991

For sale by the National Technical Information Service, Springfield, Virginia 22161-2171